



A higher-order-mode fiber delivery for Ti:Sapphire femtosecond lasers

Jespersen, Kim Giessmann; Le, Tuan; Grüner-Nielsen, Lars Erik; Jakobsen, Dan; Pedersen, Martin Erland Vestergaard; Smedemand, Mikkel B.; Keiding, Søren; Palsdottir, Bera

Published in:
Optics Express

Link to article, DOI:
[10.1364/OE.18.007798](https://doi.org/10.1364/OE.18.007798)

Publication date:
2010

Document Version
Publisher's PDF, also known as Version of record

[Link back to DTU Orbit](#)

Citation (APA):
Jespersen, K. G., Le, T., Grüner-Nielsen, L. E., Jakobsen, D., Pedersen, M. E. V., Smedemand, M. B., Keiding, S., & Palsdottir, B. (2010). A higher-order-mode fiber delivery for Ti:Sapphire femtosecond lasers. *Optics Express*, 18(8), 7798-7806. <https://doi.org/10.1364/OE.18.007798>

General rights

Copyright and moral rights for the publications made accessible in the public portal are retained by the authors and/or other copyright owners and it is a condition of accessing publications that users recognise and abide by the legal requirements associated with these rights.

- Users may download and print one copy of any publication from the public portal for the purpose of private study or research.
- You may not further distribute the material or use it for any profit-making activity or commercial gain
- You may freely distribute the URL identifying the publication in the public portal

If you believe that this document breaches copyright please contact us providing details, and we will remove access to the work immediately and investigate your claim.

A higher-order-mode fiber delivery for Ti:Sapphire femtosecond lasers

Kim G. Jespersen^{1,*}, Tuan Le², Lars Grüner-Nielsen¹, Dan Jakobsen¹, Martin E. V. Pedersen¹, Mikkel B. Smedemand³, Søren R. Keiding³, Bera Palsdottir¹

¹OFS Fitel Denmark, Priorparken 680, 2605 Broendby, Denmark

²Femtolasers Produktions GmbH, Vienna, Austria

³Department of Chemistry, University of Aarhus, Langelandsgade 140, DK-8000 Aarhus C, Denmark

*kjaspersen@ofsoptics.com

Abstract: We report the first higher-order-mode fiber with anomalous dispersion at 800nm and demonstrate its potential in femtosecond pulse delivery for Ti:Sapphire femtosecond lasers. We obtain 125fs pulses after propagating a distance of 3.6 meters in solid-silica fiber. The pulses could be further compressed in a quartz rod to nearly chirp-free 110fs pulses. Femtosecond pulse delivery is achieved by launching the laser output directly into the delivery fiber without any pre-chirping of the input pulse. The demonstrated pulse delivery scheme suggests scaling to >20meters for pulse delivery in harsh environments not suited for oscillator operation or in applications that require long distance flexibility.

©2010 Optical Society of America

OCIS codes: (320.0320) Ultrafast optics; (060.2310) Fiber optics

References and links

1. W. R. Zipfel, R. M. Williams, and W. W. Webb, "Nonlinear magic: multiphoton microscopy in the biosciences," *Nat. Biotechnol.* **21**(11), 1369–1377 (2003).
 2. B. A. Flusberg, E. D. Cocker, W. Piyawattanametha, J. C. Jung, E. L. M. Cheung, and M. J. Schnitzer, "Fiber-optic fluorescence imaging," *Nat. Methods* **2**(12), 941–950 (2005).
 3. D. G. Ouzounov, K. D. Moll, M. A. Foster, W. R. Zipfel, W. W. Webb, and A. L. Gaeta, "Delivery of nanojoule femtosecond pulses through large-core microstructured fibers," *Opt. Lett.* **27**(17), 1513–1515 (2002).
 4. T. Le, G. Tempea, Z. Cheng, M. Hofer, and A. Stingl, "Routes to fiber delivery of ultra-short laser pulses in the 25 fs regime," *Opt. Express* **17**(3), 1240–1247 (2009).
 5. S. Ramachandran, M. F. Yan, J. Jasapara, P. Wisk, S. Ghalimi, E. Monberg, and F. V. Dimarcello, "High-energy (nanojoule) femtosecond pulse delivery with record dispersion higher-order mode fiber," *Opt. Lett.* **30**(23), 3225–3227 (2005).
 6. F. Luan, J. C. Knight, P. St. J. Russell, S. Campbell, D. Xiao, D. T. Reid, B. J. Mangan, D. P. Williams, and P. J. Roberts, "Femtosecond soliton pulse delivery at 800nm wavelength in hollow-core photonic bandgap fibers," *Opt. Express* **12**(5), 835–840 (2004).
 7. J. S. Skibina, R. Iliev, J. Bethge, M. Brock, D. Fischer, V. I. Beloglasov, R. Wedell, and G. Steinmeyer, "A chirped photonic-crystal fibre," *Nat. Photonics* **2**(11), 679–683 (2008).
 8. S. Ramachandran, S. Ghalimi, J. W. Nicholson, M. F. Yan, P. Wisk, E. Monberg, and F. V. Dimarcello, "Anomalous dispersion in a solid, silica-based fiber," *Opt. Lett.* **31**(17), 2532–2534 (2006).
 9. M. Schultz, O. Prochnow, A. Ruehl, D. Wandt, D. Kracht, S. Ramachandran, and S. Ghalimi, "Sub-60-fs ytterbium-doped fiber laser with a fiber-based dispersion compensation," *Opt. Lett.* **32**(16), 2372–2374 (2007).
 10. J. W. Nicholson, S. Ramachandran, and S. Ghalimi, "A passively-modelocked, Yb-doped, figure-eight, fiber laser utilizing anomalous-dispersion higher-order-mode fiber," *Opt. Express* **15**(11), 6623–6628 (2007).
 11. L. Grüner-Nielsen, S. Ramachandran, K. Jespersen, S. Ghalimi, M. Garmund, and B. Palsdottir, "Optimization of higher order mode fibers for dispersion management of femtosecond fiber lasers," *Proc. SPIE, Fiber Lasers V: Technology, Systems, and Applications*, 6873_25 (2008).
 12. S. Ramachandran and M. F. Yan, "Static and tunable dispersion management with higher order mode fibers", in *Fiber Based Dispersion Compensation*, S. Ramachandran, ed. (Springer, New York, 2007).
 13. D. Müller, J. West, and K. Koch, "Interferometric chromatic dispersion measurement of a photonic band-gap fiber", *Proc. SPIE, Active and passive optical components for WDM communications II*, 4870, 395 (2002).
 14. S. Ramachandran, Z. Wang, and M. Yan, "Bandwidth control of long-period grating-based mode converters in few-mode fibers," *Opt. Lett.* **27**(9), 698–700 (2002).
 15. C. Schmidt, S. Galmi, P. Balling, S. Ramachandran, and J. W. Nicholson, "Enhanced resolution in nonlinear microscopy using the LP₀₂ mode of an optical fiber", accepted for *The Conference on Lasers and Electro-Optics (CLEO)* (2010).
-

1. Introduction

Fiber optic delivery of femtosecond laser pulses is attractive due to several reasons. High flexibility combined with a diffraction limited output are valuable properties in e.g. confocal and multiphoton microscopy [1]. Moreover, a fiber delivery enables pulse delivery at places difficult to reach using conventional mirrors and lenses such as in endoscopic multiphoton microscopy, which is an emerging medical diagnostic tool for in-vivo imaging [2]. On the laser side, the femtosecond Ti:Sapphire laser has been the chosen femtosecond laser due to its versatile performance and high pulse quality. This has resulted in a wealth of scientific and technological applications of ultrafast technologies based on the Ti:Sapphire laser in the last two decades. The Ti:Sapphire laser is a photon oscillator composed of free-space bulk optic components giving the laser high pulse-to-pulse repeatability and low timing jitter. However, as strong as the performance is, the Ti:Sapphire laser is suffering from a delicate alignment of the bulk-optic oscillator. This poses practical limitations to the operation environment. Some improvements have been made to adapt the Ti:Sapphire laser for industrial applications, however, a golden solution to eliminate the environmental influence has still to come. A promising route for Ti:sapphire femtosecond lasers to gain industrial market shares is to employ fiber based pulse delivery that allows the operator to access femtosecond pulses in harsh environments while the oscillator is installed in a less demanding environment. Hence, a fiber delivery adds significant value to the Ti:Sapphire femtosecond laser in industrial applications.

The key challenge in a fiber based pulse delivery for Ti:Sapphire femtosecond lasers are the dispersive and nonlinear properties inherent to fiber technology. The characteristic length scales involved are the dispersion length, L_D , and nonlinear length, L_{NL} :

$$L_D = \frac{2\pi c T_0^2}{\lambda^2 |D|}, \quad L_{NL} = \frac{\lambda A_{eff}}{2\pi n_2 P_0},$$

where λ is wavelength, T_0 is pulse width ($T_{FWHM} \approx 1.763 T_0$, *sech*² pulse), D is dispersion, A_{eff} is the effective area, n_2 is the nonlinear index, and P_0 is the pulse peak power. Note that the dispersion, D , is related to the group velocity dispersion, β_2 , by $D = -2\pi c \beta_2 / \lambda^2$. Linear pulse propagation is obtained when $L_D \ll L_{NL}$ i.e. the impact of nonlinear effects is negligible. For solid core fibers the inequality implies that the product $|D| \cdot A_{eff}$ is the crucial material figure of merit.

Several interesting fiber delivery schemes have been demonstrated in literature. In one category are the normal dispersive fibers such as traditional large mode area (LMA) fibers, microstructured endlessly single mode LMA fibers [3,4], and higher-order-mode (HOM) fibers [5]. They have either large mode fields (equivalent to a large effective area) or high dispersion to operate in a regime where $|D| \cdot A_{eff}$ is large and $L_D \ll L_{NL}$. Hence reducing the impact of nonlinear effects. However, since they are normal dispersive they all require some sort of pre-chirping to provide a fourier transform limited output at the end of a fiber delivery. Usually this is done by bulk optic gratings or prisms or combinations hereof. A particular drawback associated with solid silica LMA fibers is a high bend loss which makes them less suited for fiber delivery. A second category of potential delivery fibers are air-guiding fibers, which have a small n_2 in order to minimize the effect of nonlinearities and to enable high power applications. These are the so-called hollow core photonic band gap (PBG) fibers with anomalous dispersion [6] and chirped photonic band gap (CPBG) fibers with zero dispersion and zero dispersion slope [7]. Although both fiber types are intriguing due to a large nonlinear length they do have critical drawbacks such as a large positive dispersion slope and high transmission loss, respectively. When implementing such fibers in fiber deliveries one is forced to compromise on the system performance in terms of fiber length.

A different approach to fiber delivery of ultra short pulses is to focus on low power applications and simultaneously eliminate the need for pulse pre-chirping as mentioned above. A fiber delivery based on alternating sections of normal and anomalous dispersive

fibers would do just that. Moreover, such a delivery scheme has the potential of scaling to long distance pulse delivery. So far anomalous dispersive fibers in the 800nm wavelength region are represented by hollow core PBG fibers and index guiding microstructured fibers. Hollow core fibers have typically large and positive dispersion slopes which will result in significant accumulation of higher order dispersion when combined with normal dispersive single mode fiber, which also have positive dispersion slope. Index guiding microstructured fibers with anomalous dispersion at 800nm have in general small effective areas, A_{eff} . They are essentially highly nonlinear fibers and therefore not suited for pulse delivery.

In this work we present a HOM fiber with anomalous dispersion at 770nm and which has an effective area that is comparable to single mode fibers. Furthermore, it has partly dispersion slope matching to normal dispersive single mode fibers. The HOM fiber is included in a fiber module having both, normal and anomalous dispersion fiber sections with net zero group delay dispersion. We propose its application in long distance femtosecond pulse delivery for Ti:Sapphire femtosecond lasers. A Ti:Sapphire pulse delivery is demonstrated, in which 125fs pulses are propagated over a fiber distance of 3.6m by launching the laser output directly into the delivery fiber without any pre-chirping of the input pulse.

2. Higher-order-mode fiber with anomalous dispersion at 800nm

Ramachandran et al. [8] have demonstrated anomalous dispersion at 1 μ m in a solid-silica fiber device using a design based on HOM propagation. Conversion between the HOM LP₀₂ and fundamental mode LP₀₁ was made by long-period gratings (LPG). Such a device was successfully implemented as a dispersion controlling element inside various types of mode locked Ytterbium fiber lasers [9–11], and as pulse compressing fiber delivery with sub-100fs output [10]. Here we present a HOM device for operation around 800nm. The design of HOM fibers with anomalous dispersion at 800 nm is more challenging compared to the 1 μ m wavelength region due to the fact that the normal material dispersion is higher at 800nm, and therefore more waveguide dispersion is needed at 800 nm compared to 1 μ m.

The HOM fiber is a few-mode fiber with a triple cladding index profile. The index profile is chosen such that the difference between the LP₀₂ propagation constant and the next HOM propagation constant is kept sufficiently large to suppress unwanted mode coupling. This has previously been shown by L. Grüner-Nielsen et al. [11] to compromise the amount of anomalous dispersion that can be obtained and hence a trade off exists. In practice the trade off sets an upper limit to the dispersion. A second critical design issue is to facilitate broad band mode conversion in LPG's. A comprehensive description of broad band mode conversion in HOM fibers can be found in [12]. A broad wavelength range is required in the context of femtosecond pulses.

Anomalous dispersion is obtained even though silica exhibits a large normal material dispersion in the near infrared. The material dispersion of silica is compensated by anomalous waveguide dispersion of the HOM. In Fig. 1 the dispersion curves of the LP₀₁ and LP₀₂ modes and the single mode fiber (SMF) ClearLite 780-11 (OFS product), are shown. The dispersion of the LP₀₁ and LP₀₂ modes is calculated from the index profile of the relevant preform position using a scalar mode solver. Furthermore, all dispersion curves are experimentally verified using a white light interferometer based on a supercontinuum source (SuperK, Koheras) [13].

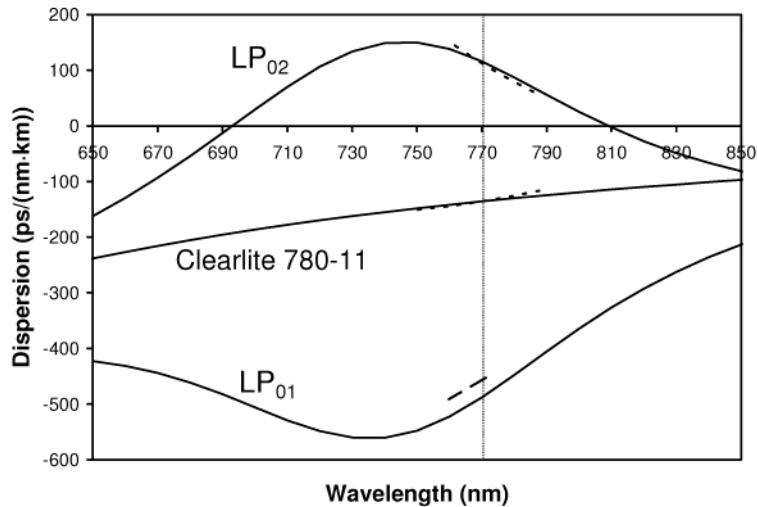


Fig. 1. Dispersion curves as calculated from the refractive index profile of the fiber preform of LP₀₂ HOM and LP₀₁ fundamental mode. Also shown is the calculated dispersion of the single mode fiber ClearLite 780-11. Dotted curves are corresponding dispersion curves measured with a white light interferometer.

The center wavelength of the anomalous dispersion fiber is set by the wavelength for optimum mode conversion (indicated by a vertical dotted line in Fig. 1). In this case broad band mode conversion is obtained in a 20nm wavelength range around 770nm. The HOM LP₀₂ dispersion at 770nm is found to be $D = +112.7\text{ps}/(\text{nm}\cdot\text{km})$ ($\beta_2 = -0.0355\text{ps}^2/\text{m}$) with a calculated dispersion slope of $S = -2.542\text{ps}/(\text{nm}^2\cdot\text{km})$. This corresponds to a third order dispersion (TOD) of $\beta_3 = -0.0002229\text{ps}^3/\text{m}$. The fundamental LP₀₁ mode has a high normal dispersion of $D = -456.9\text{ps}/(\text{nm}\cdot\text{km})$ ($\beta_2 = +0.144\text{ps}^2/\text{m}$) due to the combination of high material dispersion and high normal waveguide dispersion. For comparison the dispersion of the SMF at 770nm is measured to be $D = -135.71\text{ps}/(\text{nm}\cdot\text{km})$ ($\beta_2 = +0.0427\text{ps}^2/\text{m}$). The SMF dispersion slope and TOD are $S = +0.591\text{ps}/(\text{nm}^2\cdot\text{km})$ and $\beta_3 = +0.0000236\text{ps}^3/\text{m}$, respectively. The SMF is a match-clad fiber type with a dispersion dominated by the material dispersion of silica. The dispersion of the LP₀₂ and the SMF are approximately of the same magnitude with opposite sign. Furthermore, it is seen that the dispersion slopes are of opposite sign such that when combining fiber sections of LP₀₂ and SMF the higher order dispersion is partly compensated.

The effective area of the HOM is calculated from preform data to be $14.9\mu\text{m}^2$ at 770nm. For comparison the effective area in index guiding microstructured fibers with anomalous dispersion in the near infrared is of the order of $2\text{--}5\mu\text{m}^2$. The relatively larger effective area means that the non-linear length can be increased 3-8 times (assuming similar dispersion values) by using the proposed anomalous dispersion fiber and still obtain linear pulse propagation. Experimental data presented below show that nearly dispersive pulse propagation can be expected for input pulses with 75fs pulse duration and 85pJ pulse energy. At higher pulse energies propagation in the soliton regime could be exploited to provide pulse delivery or wavelength tunability through the Raman shift, and at even higher energies generation of supercontinuum.

A solid-silica fiber module is assembled using the anomalous dispersion HOM fiber and sections of SMF. Figure 2 shows a diagram of such a fiber module. The module is similar to what has been published previously for the $1\mu\text{m}$ wavelength regime [8]. It is a symmetric module consisting of two LPG mode converters separated by a section of HOM fiber.

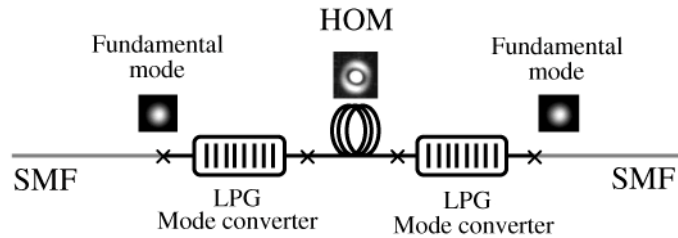


Fig. 2. Solid-silica fiber module for femtosecond pulse delivery.

Mode conversion is provided by 5mm LPG's inscribed directly into the few mode fiber using hydrogen loading and UV irradiation. The mode converters include an LPG as well as a mode matched splice to SMF. From the mode matched splice to the LPG the light propagates in the LP_{01} mode. Both mode converters are pigtailed with single mode fiber to allow easy implementation in existing fiber assemblies. The length of the HOM fiber relative to the single mode pigtail fibers can be varied to obtain a net dispersion that meets the requirements of a specific application. In the present fiber delivery demonstration the length of the single mode pigtail fibers were trimmed such that the complete fiber length was 3.6m with a net group delay dispersion close to zero.

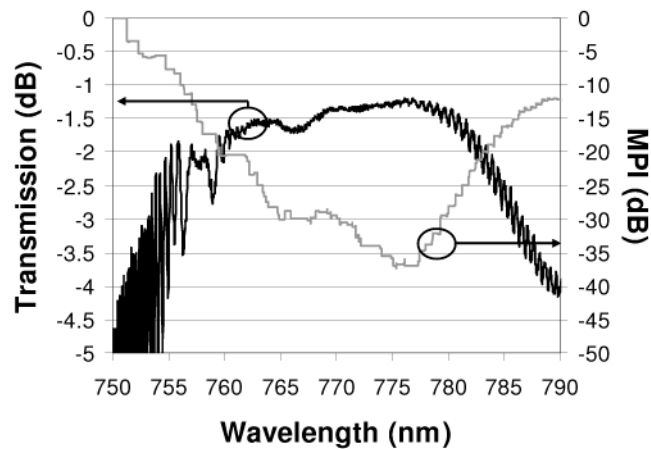


Fig. 3. Transmission and MultiPath Interference (MPI) calculated in 3nm wavelength intervals.

LPG's with a peak conversion efficiency of approximately 30dB and an efficiency of more than 15dB across a 20nm bandwidth were used to assemble the module. A conversion efficiency of 30dB corresponds to 99.9% of the mode being converted. In the case of a non-ideal mode conversion the fiber module represents a Mach-Zender interferometer where the two paths are the LP_{01} and LP_{02} propagation modes (assuming that only two modes are present). The associated interference, called multipath interference (MPI), appears in the transmission spectrum of the module as periodic ripple. The MPI can be calculated from the peak-to-peak values of the ripple. For the current module MPI is measured to be less than -27dB over a 16nm bandwidth (see Fig. 3). For a femtosecond pulse propagating through the module this means that the ratio of the energy contained in the pulse to the energy contained in a pedestal is better than 500:1. In practice, the MPI depends critically on HOM fiber to HOM fiber splices. The insertion loss of the fiber module is approximately 1.5dB in a 20nm operation bandwidth centered at 770nm. The loss is mainly due to splice loss. The transmission loss in the HOM fiber itself is estimated to be < 10dB/km. The transmission spectrum of the complete module as well as the MPI property calculated in 3nm intervals is shown in Fig. 3.

In general the performance of the HOM module with anomalous dispersion at 800nm is found to be comparable to that of similar devices operating in the 1 μ m wavelength regime.

The differences are, however, a less broad operation bandwidth and a slightly higher MPI value. In the 1 μ m wavelength regime operation bandwidths of 30-40nm can be obtained routinely, and the MPI is low in a broader wavelength range. It can be shown that the bandwidth of the LPG is inversely proportional to the square root of the difference in dispersion between LP₀₁ and LP₀₂ times the LPG length, $\Delta\lambda \sim 1/(\Delta D \cdot \text{LPG length})$ [14]. Since the dispersion difference is higher at 800nm in the current design than at 1 μ m, the bandwidth is reduced. An obvious modification to the module in order to increase the bandwidth would be to reduce the LPG length. The LPG length dependence suggests that by reducing the LPG length e.g. from the current 5mm to 2.5mm one can expect an increase in bandwidth by a factor of $\sqrt{2}$ i.e. ~28nm compared to the current ~20nm.

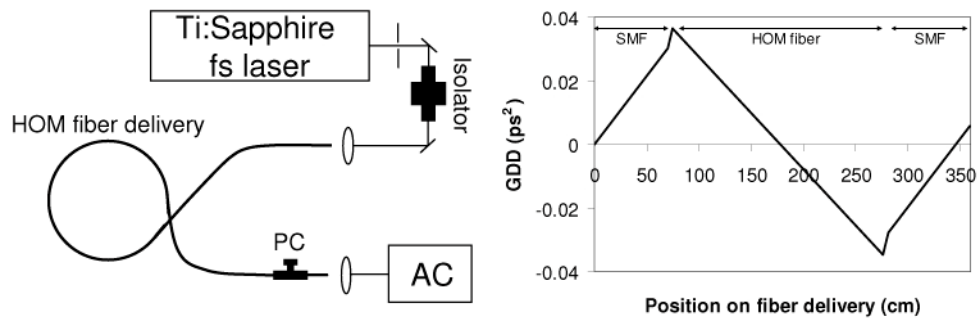


Fig. 4. Left: Ti:Sapphire femtosecond laser with a 3.6m fiber delivery. PC is polarization control and AC is a fringe resolved autocorrelator. Right: Dispersion map of fiber delivery.

3. Ti:Sapphire fiber delivery based on higher order mode fiber

The HOM fiber with anomalous dispersion at 800nm is demonstrated in a fiber delivery for a Ti:Sapphire femtosecond laser. The laser is a modified Integral laser from Femtolasers. The laser had 10nm FWHM spectral bandwidth centered at 770nm and provided >100mW average output power with a pulse repetition rate of 82MHz. A diagram of the Ti:Sapphire femtosecond laser with HOM fiber delivery is shown in Fig. 4 (left) together with the measured dispersion map of the fiber delivery (right). An optical isolator was included to prevent feedback into the oscillator from the fiber coupling (flat fiber cleave). This can potentially be eliminated using angled fiber coupling. The FWHM pulse duration after the optical isolator was 75fs. Coupling into and out of the fiber was done with two achromatic lenses. The launched power was varied using a pinhole in the free-space section and/or by detuning the fiber coupling. To obtain a pulse delivery with approximately zero net group delay dispersion we assembled a 3.6m long fiber delivery consisting of three sections of fiber with alternating dispersion sign. This leads to a fiber delivery that can be implemented directly at the output of the Ti:Sapphire laser without the need for addition pre-chirping with bulk optical components. Pulse diagnostics at the fiber output is made by a fringe resolving autocorrelator and a spectrometer. A polarization control is included to match the state of polarization to the orientation of the nonlinear crystal in the autocorrelator.

The fiber delivery provides femtosecond pulses with a pulse duration of 125fs (FWHM) at the fiber output. The pulse duration could be further reduced by fine tuning of the net group delay dispersion using a 10cm piece of quartz rod following the fiber output. The resulting pulse delivery performance is shown in Fig. 5. After fine tuning of the group delay dispersion we obtained a nearly chirp-free femtosecond pulse with FWHM pulse duration of 110fs. The pulse duration is calculated by $\tau_p = \tau_{AC} / B$, where τ_{AC} is the FWHM of the fringe resolved autocorrelation trace, and B is the deconvolution factor for a sech^2 pulse (1.897). The delay between the pulses in the autocorrelator was varied up to approximately 2ps to look for signs of a pedestal. However, no change in the background signal could be detected. This leads us to the conclusion that the delivered pulses are nearly chirp-free. The peak power could be increased up to 0.4kW, as measured at the fiber output and 0.5kW after the quartz rod. The

corresponding peak power at the input of the fiber delivery was 1.0kW. Above this value self phase modulation was seen to broaden the pulse spectrum significantly. Moreover, since the LPG mode converters are acting as spectral filters at wavelengths exceeding the LPG bandwidth, an increase in input power resulted in side-lobe formation in the autocorrelation trace and in an increased insertion loss.

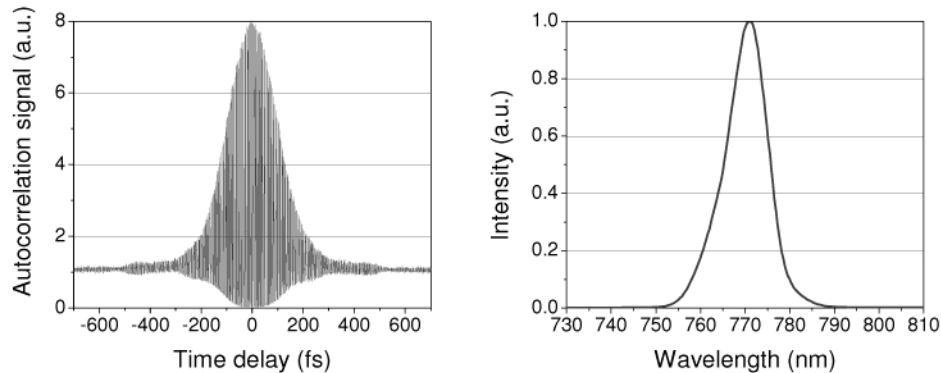


Fig. 5. Fringe resolved autocorrelation and spectrum of the fiber delivery output. The FWHM pulse duration is 110fs, and the fiber delivery is a 3.6m solid-silica HOM fiber module.

The use of a 10cm quartz rod following the fiber output implies that the final pulse compression is made partly in quartz with a collimated beam. This corresponds roughly to the conditions of an actual imaging setup with a femtosecond fiber delivery. In this case the final pulse compression is considered to take place in the microscope objective, which like the quartz rod will have normal dispersion. In the present demonstration the output pulse was 125fs and down-chirped. However, by addition of a section of normal dispersive SMF the final pulse compression could likewise occur within the fiber assuming linear pulse propagation. In this case, we expect an output pulse duration similar to what is observed following the quartz rod, i.e. 110fs. On the other hand, if the final pulse compression is not linear but has a significant nonlinear contribution we would expect pulse broadening due to spectral narrowing. However, no significant change of the measured pulse duration could be seen when the output power was further reduced. Moreover, since the dispersion map has a zero crossing at roughly 1.8m where the pulse is going from being up-chirped to being down-chirped, the pulse has already the shortest possible pulse duration within the HOM fiber (see Fig. 4). Therefore, since the ratios L_D / L_{NL} are approximately the same in the HOM fiber and in the SMF at the fiber output, we expect this particular position to be an indicator for linear pulse propagation. In this respect the quartz rod was simply implemented to achieve the shortest pulse duration. It probably could have been replaced by lengthening the SMF accordingly without any impact on the results of the measurements.

At the best pulse delivery performance the fiber assembly consisted of 201.2cm HOM fiber with light propagation in the LP_{02} mode, and SMF pigtail fiber on either side to balance the group delay dispersion. The SMF lengths were 70.5cm (at the input) and 78.4cm (at the output). The output was propagated additional 10cm in a quartz rod as described above. The fiber sections are separated by broadband LPG mode converters that couple light between the LP_{01} and LP_{02} mode. Each mode converter contains a short section of HOM fiber where the light propagates in LP_{01} . The short sections of LP_{01} were 4.5cm and 4.9cm. The net group delay dispersion and the accumulated TOD of the fiber delivery were $+0.00574\text{ps}^2$ ($\sum \beta_2 l$) and $-38.9 \cdot 10^{-5}\text{ps}^3$ ($\sum \beta_3 l$) (excluding 10cm quartz rod). Here we used the measured dispersion values and the calculated dispersion slope values. We notice that the group delay dispersion is slightly offset from the assumption that zero net group delay dispersion should provide the shortest possible pulse. However, taking the uncertainty of the dispersion measurement into account as well as a potential contribution from nonlinear pulse propagation this discrepancy

is to be expected. The fact that the output spectrum is slightly asymmetric could indicate that the pulse propagation is only approximately linear (see Fig. 5).

4. Discussion

The results presented above show that the pulse delivery has approximately linear pulse propagation over 3.6m when the input pulse energy is less than 85pJ and the input pulse duration is at least 75fs. Thus, the limiting peak power at the fiber input is 1.0kW. The peak power at the fiber output is lower mainly due to insertion loss, residual chirp, and accumulated higher order dispersion such that the corresponding output peak power is 0.4kW (125fs pulses with 61pJ pulse energy). After fine tuning of the group delay dispersion using a quartz rod, a nearly chirp-free pulse is obtained with a peak power of 0.5kW. The fact that the HOM fiber and SMF have only partly compensating dispersion slopes results in a significant amount of accumulated TOD, limiting the final pulse duration. From a fiber design perspective it is possible to improve the dispersion slope match and thereby to reduce the pulse duration at the fiber output. The power level achieved in the present demonstration is slightly on the low side for endoscopic diagnostic applications or terahertz generation, which are two important applications that would benefit from a fiber delivery at 800nm. Especially when taking into account additional loss introduced by optics belonging to a given application subsequent to the fiber delivery. The demonstration, however, shows the potential of the HOM fiber delivery for low power applications.

In general linear pulse propagation requires $L_D \ll L_{NL}$, as mentioned in the introduction. In the demonstrated fiber delivery the ratio L_D / L_{NL} is approximately 0.5 in the relevant fiber sections. That is, at the fiber input, in the central HOM fiber section where the pulse is compressed, and at the fiber output. Thus the fiber delivery is operated close to the point where nonlinear effects become relevant. The power performance depends critically on the product $|D| \cdot A_{eff}$ suggesting that there are basically two ways for improvement. Both, the effective area and the dispersion can be increased to some extent by shifting the operation wavelength of the HOM fiber to 800nm. Another approach in order to improve the power performance is to modify the dispersion map such that no central pulse compression within the fiber delivery occurs. Hence, the pulse will be shortest only at the fiber launch and exit. Simulations indicate that this will increase the power performance by one order of magnitude. This would make the presented fiber delivery suitable for several low power applications. The price one has to pay is an LP_{02} output mode rather than a Gaussian mode. For many applications it may be a good solution. However, further studies on the focusing properties in applications involving linear and nonlinear excitation are needed to determine the real applicability of such an alternative dispersion map [15]. Another possibility is to write an LPG directly at the fiber output in order to convert the LP_{02} mode to the fundamental mode prior to leaving the fiber delivery.

The demonstration of an approximately linear pulse propagation presented in this paper, opens up new opportunities for femtosecond pulse delivery. We expect short pulse fiber deliveries directly from the output of the Ti:Sapphire laser over 20-50m to be a real possibility, and future experiments will target such a demonstration. The delivery distance will mainly be limited by the accumulated higher order dispersion. A long distance fiber delivery of >20m would enable femtosecond pulse application in harsh environments while the Ti:Sapphire oscillator is located in a separate and less demanding environment. Another scenario suited for a >20m long fiber delivery could be an application that requires long distance flexibility or even a portable laser.

5. Conclusion

In conclusion we have presented a solid-silica HOM fiber delivery for Ti:Sapphire femtosecond lasers. The fiber delivery is based on a HOM fiber with anomalous dispersion at 770nm and facilitates pulse delivery directly from the output of the laser without the need for pre-chirping of the femtosecond pulse by additional optics. We have demonstrated a femtosecond Ti:Sapphire laser with a 3.6m HOM fiber delivery and obtain 125fs pulses at the

fiber output. The output could be further compressed in a quartz rod to obtain a nearly chirp-free 110fs pulse. The optical power available after the fiber delivery in the current demonstration was 61pJ within 125fs fs corresponding to 0.4kW peak power.

The fiber module used for pulse delivery includes a HOM fiber with anomalous dispersion at 770nm. The module consists of SMF-HOM-SMF fiber sections to obtain zero net group delay dispersion. The dispersion of the HOM is +112.7 ps/(nm·km), which is comparable to that of single mode fibers at 800nm with opposite sign. The dispersion slope is negative and provides partly compensation of the dispersion slope in single mode fibers (positive slope) when used together.

The pulse delivery demonstration suggests femtosecond pulse delivery over what can be considered extreme distances (>20m) in the context of femtosecond pulse propagation. A long fiber delivery for femtosecond pulses will improve the flexibility of Ti:Sapphire femtosecond lasers and add new possibilities in industrial applications.

Acknowledgements

We greatly acknowledge Martin Garmund and Turid Solvang at OFS Fitel Denmark for writing long-period gratings used in this study.